NEOPLASMA accepted, ahead of print version;
Cite article as https://doi.org/10.4149/neo_2020_190706N600

Running title: Effect of LncRNA-LINC00261 in NSCLC

LncRNA-LINC00261 suppresses the progression of NSCLC cells through upregulating miR-19a-mediated Kruppel-like factor 2 (KLF2)

Z.Y. LI[1#], Z.Z. LI[1#], J.H. ZHOU[1]*, Z.J. ZHONG[1], X.J. WANG[2], L. ZHONG[3], W.Y. ZHOU[4]*

[1]Department of Pathology, The 5th Affiliated Hospital of Sun Yat-sen University, Zhuhai, China; [2]Department of Cardiothoracic Surgery, The 5th Affiliated Hospital of Sun Yat-sen University, Zhuhai, China; [3]Department of Pathology, The 2nd Affiliated Hospital of Guangzhou Medical University, Guangzhou, China; [4]Department of Central Laboratory, The 5th Affiliated Hospital of Sun Yat-sen University, Zhuhai, China

***Correspondence:** okdkaf@163.com, zhouwenying78056@sina.com
[#]Contributed equally as co-first authors

Received July 6, 2019 / Accepted November 13, 2019

Long non-coding RNA LINC00261 (LINC00261) has been reported to be implicated in tumorigenesis, treatment, and prognosis in different cancers including non-small cell lung cancer cells (NSCLCs). However, its mechanisms have been poorly investigated in NSCLC. Expressions of LINC00261, miR-19a and Kruppel-like factor 2 (KLF2) were detected using RT-qPCR and western blotting. Cell viability, migration and invasion and apoptosis were detected by MTT assay, transwell assay, flow cytometry and the expressions of Bcl-2, Bax, and cleaved caspase 3 were analyzed by western blotting. Tumor growth in vivo was measured in a xenograft experiment. The target binding between miR-19a and LINC00161 or KLF2 was predicted on the miRcode or Targetscan website and confirmed by luciferase reporter assay. The results showed that LINC00261 was downregulated in NSCLC tumors and cell lines, and this downregulation was correlated with higher TNM stage, larger tumor size, lymph node metastasis, and poor prognosis. Functionally, the upregulation of LINC00261 could promote NSCLC cell apoptosis and inhibit cell viability, migration, and invasion in A549 and H1299 cells, as well as suppress tumor growth. Mechanically, LINC00261 positively regulated KLF2 expression in NSCLC tumors through sponging miR-19a. Expression of miR-19a was upregulated while KLF2 was downregulated in NSCLC tumors, and there existed a negative linear correlation between miR-19a and LINC00261 or KLF2. Rescue experiments demonstrated that both miR-19a upregulation and KLF2 downregulation could abolish the LINC00261 effect in A549 and H1299 cells. Collectively, the upregulation of LINC00261 suppressed NSCLC cell progression through upregulating miR-19a-mediated KLF2, suggesting LINC00261/miR-19a/KLF2 pathway could contribute to the initiation, development, and prognosis in NSCLC.

Key words: LINC00261; miR-19a; KLF2; NSCLC

Non-small cell lung cancer (NSCLC) is one of the most lethal cancers in the worldwide and represents the most common subtype of lung cancer that accounts for approximately 85% [1, 2]. NSCLC is classified into three different subtypes: squamous cell carcinoma, adenocarcinoma, large cell carcinoma. Due to the limitations of early diagnostic techniques and the lack of early specific clinical manifestations, 70-80% of patients are diagnosed at advanced stages [2]. Most patients with NSCLC present with metastatic disease and the five-year survival rate of lung cancer is less than 20% [3]. In spite of the continuous researches updating in NSCLC, the poor of early diagnosis and effective treatment is also the major cause of the rising incidence of lung cancer [4]. Therefore, it is essential to further investigate the molecular events accompanying the progression of lung cancer, especially NSCLC.

Long non-coding RNAs (lncRNAs) are longer than 200 nucleotides in length and lack protein coding potential. LncRNAs can regulate biological processes via diverse molecular mechanisms, for instance sponges for miRNAs [5]. The association of lncRNAs with cancer has been well-summarized and the potential of lncRNA-based cancer therapy has been pointed out [6]. Various studies have suggested the dysregulation of lncRNAs in NSCLC and their role in progression of NSCLC cells such as proliferation, apoptosis, migration, invasion, *etc.* [7]. Moreover, the association between lncRNAs and drug resistance has also been confirmed [8]. In addition, specific lncRNAs are revealed to exert potential functions in NSCLC subtypes [9]. Therefore, there emerging evidence shows that lncRNAs can function as biomarkers for diagnosis and prognosis in NSCLC [10].

LncRNA-LINC00261 (LINC00261) is originally identified as definitive endoderm-associated lncRNA1 (DEANR1), and its highly expression drives the endoderm differentiation. Recently, LINC00261 is supposed to be complicated in various cellular processes in cancers, including lung cancer [11], esophageal cancer [12], gastric cancer [13]. In lung cancer, LINC00261 is downregulated and acts as an epigenetically-regulated tumor suppressor in NSCLC. Decreased expression of LINC00261 has been suggested to be a prognostic marker for patients with NSCLC [11]. It was reported that LINC00261 and the adjacent gene FOXA2 were closely related to epithelial-to-mesenchymal transition (EMT), cell cycle arrest and DNA damage pathway in lung adenocarcinoma [14, 15]. Very recently, LINC00261 was announced to suppress cell proliferation

and metastasis by downregulating Snail expression via EMT [16]. However, the role and mechanism underlying the tumor-suppressive role of LINC00261 remain to be largely uncovered in NSCLC.

The competing endogenous RNA (ceRNA) network including lncRNAs, microRNAs (miRNAs) and message RNAs (mRNAs) has been well-documented in cancers [17] including lung cancer [18]. Comprehensive analysis of LINC00261-associated ceRNA net has been announced in tongue squamous cell carcinoma and endometrial carcinoma [19, 20]. However, the outcomes in this field remain disappointed, especially in lung cancer. In this study, we investigated the dysregulation of LINC00261 in tumor tissues from patients with NSCLC and NSCLC cell lines. Functional experiments were carried out to evaluate the role of LINC00261 in NSCLC cell viability, apoptosis, migration and invasion *in vitro*, as well as the tumor growth *in vivo*. More importantly, LINC00261/miRNA/mRNA pathway was further identified.

Materials and Methods.

Acquirement of tissue samples. With approval of Research Ethics Committee of the Fifth Affiliated Hospital of Sun Yat-sen University and the written informed consents from 62 NSCLC patients from 2013 to 2017. All patients were with primary NSCLC and excluded treatment of radiotherapy or chemotherapy before surgery. Paired NSCLC tumor tissues and adjacent normal tissues were obtained at the Fifth Affiliated Hospital of Sun Yat-sen University and immediately frozen in liquid nitrogen and then stored at -80 °C. A small aliquot of the tumor tissues and adjacent normal tissues was immunohistochemically confirmed. The diagnosis of all patients was confirmed by two pathologists and the clinical features of all enrolled patients were shown in Table 1.

Cells and cell culture. Normal human bronchial epithelium cell line BEAS-2B (CRL-9609), human embryonic kidney cell line HEK293T (CRL-3216) and human NSCLC cell lines A549 (CCL-185), H1299 (CRL-5803) and SK-MES-1 (HTB-58) cells were purchased from American Type Culture Collection (ATCC; Manassas, USA). PC-9 cells (RCB4455) were obtained from RIKEN Cell Bank (Koyadai, Tsukuba, Ibaraki, Japan). Except for HEK293T cells, all other cells were cultured in RPMI-1640 medium (Hyclone, Logan, USA) and HEK293T cells were cultivated in Dulbecco's Modified Eagle's Medium (DMEM; Hyclone). All cultured cells were in medium containing 10% fetal bovine serum (FBS; Hyclone) and 1% penicillin/streptomycin (Invitrogen,

Carlsbad, USA) at 37 °C with 5% CO_2.

Cell transfection. For overexpression, miR-19a mimics and miR-NC mimics were obtained from GenePharma (Shanghai, China) and LINC00261 was cloned into pcDNA 3.1 (Invitrogen, Carlsbad, USA). For knockdown, miR-19a inhibitors and siRNA against Kruppel-like factor 2 (KLF2) (si-KLF2), and their negative controls were acquired from GenePharma. Cells were transfected of these oligonucleotides and plasmids using Lipofectamine 2000 (Invitrogen) following the standard instruction of manufacturer. Transfected cells were cultured for an additional 48 h prior to further studies except in MTT assay. The sequence of si-KLF2 was 5'-UGCUGGAGGCCAAGCCAAAUU-3', and si-NC was 5'-AUGAACGUGAAUUGCUCAAUU-3'.

MTT assay. The cell viability of A549 and H1299 cells was determined by 3-(4,5-dimethylthiazol-2-yl)-2,5 diphenyltetrazolium bromide (MTT; Sangon, Shanghai, China) staining. After transfection, 5 mg/l MTT was added to each well on 0, 24, 48 and 72 h. Subsequently, the cultures were incubated for another 4 h at 37 °C. The supernatant was aspirated, and formazan crystals were dissolved in 100 μl dimethyl sulfoxide (DMSO; Sangon). The absorbance at 450 nm was measured with SpectraMax M4 (Molecular devices, Shanghai, China). All experiments were performed in quadruplicate.

RNA extraction and Real time quantitative PCR (RT-qPCR). For examination of LINC00261, miR-19a and KLF2 mRNA expression, total RNAs from tissues and cultured cells was extracted with TRIzol reagent (Invitrogen) and the first-strand cDNA was synthesized using high capacity RNA-to-cDNA kit (Takara, Shiga, Japan). The quantitative PCR was performed with SYBR green detection (Promega, Madison, USA) and TaqMan probe (for miRNA; Roche) on ABI 7900 real-time PCR system (Promega). GAPDH mRNA was used as reference gene for LINC00261 and KLF2, and U6 small nuclear RNA (U6) was the internal control to mature miR-19a. The reactions were performed in quadruplicate for each sample at least three independent runs and the primers involved are as follows: LINC00261: 5'-GTCAGAAGGAAAGGCCGTGA-3' forward and 5'-TGAGCCGAGATGAACAGGTG-3' reversed; KLF2: 5'-CCAAAAATGCCCACCTGTCT-3' forward and 5'-GTGGCATCTTCTCTCCCACC-3' reversed [21]; GAPDH: 5'-GCTCTCTGCTCCTCCTGTTC-3' forward and 5'-ACGACCAAATCCGTTGACTC-3' reversed; miR-19a: 5'-TGTGCAAATCTATGCAAA-3' forward and 5'-GTGCAGGGTCCGAGGTATTC-3'

reversed [22]; U6: 5'-CTCGCTTCGGCAGCACA-3' forward and 5'-AACGCTTCACGAATTTGCGT-3' reversed [23].

Flow cytometry. Apoptosis rate of transfected A549 and H1299 cells was analyzed by Annexin V-FITC/PI kit (Beyotime, Shanghai, China) on flow cytometry. After transfection for 48 h, apoptotic cells were collected and were washed with phosphate-buffered saline (PBS). Cell suspension of 10^6 cells were prepared and labelled with FITC-Annexin V and Propidium Iodide (PI) for 30 min in the dark. The fluorescence was analyzed on Influx Flow Cytometer & Cell Sorter System (BD, Franklin Lakes, USA). Quadrants were positioned on Annexin V/PI plots to distinguish apoptotic cells (Annexin V+/PI-, Annexin V+/PI+). Apoptosis rate= apoptotic cells/total cells × 100%.

Western blotting. Total protein from cultured A549 and H1299 cells was isolated in RIPA lysis buffer (Beyotime, Shanghai, China) supplemented with cocktail protease inhibitor (Roche, Basel, Switzerland), and the protein concentrations were determined by Bradford protein assay reagent (Bio-Rad, Shanghai, China). Equal amounts of protein (20 μg) from each sample were loaded for the standard procedures of western blot assay. GAPDH on the same membrane was an internal standard to normalize protein levels. The primary antibodies were purchased from Cell Signaling Technology (CST; Danvers, USA) and as follows : Bcl-2 (#2872, 1:1000), Bax (#2772, 1:1000), cleaved caspase 3 (#9661, 1:1000), and GAPDH (#97166, 1:1000), antibody against KLF2 (#236507, 1:2000) was provided by Abcam (Cambridge, UK).

Transwell assay. For determination of the ability of migration and invasion, A549 and H1299 cells after transfection for 48 h were exposed with Transwell assay. Transfected cells were performed in 24-well transwell chamber (8 μm pores; Corning) with matrigel-free (for migration) or matrigel-coated (for invasion) (BD Biosciences). Transfected cells (1×10^4 cells/ml) were re-suspended into 200 μl of serum-free medium and plated in the upper chamber, and the lower chamber was filled with 500 μl complete medium containing 10 % FBS. After transwell system were stained in 37 °C for 48 h, the cells on the lower surface were stained with 0.1% crystal violet for 15 min at room temperature, followed by being photographed and counted under a light microscope.

Luciferase reporter assay. Human KLF2 mRNA (NM_016270) 3' UTR wild type and mutant type (KLF2 3' UTR-WT/MUT) was constructed into pGL4 vector (Promega). A549 and H1299

cells were co-transfected with KLF2 3' UTR-WT/MUT and miR-19a/NC mimics. All transfection procedures were performed by Lipofectamine 2000 (Invitrogen). After 48 h-transfection, the luciferase activity was measured using dual-luciferase reporter system (Promega). The ratio of firefly to renilla luciferase activity was used as the relative luciferase activity. All operations were repeated three times.

Xenograft mouse model. BALB/c nude mice (4-week-old, male, and littermate) were obtained from Model Animal Research Center of the Fifth Affiliated Hospital of Sun Yat-sen University. The mice were randomly divided into two groups (n=3). The animal experiments were approved by the Animal Care and Use Committee of the Fifth Affiliated Hospital of Sun Yat-sen University. Equal numbers (10^6) of A549 cells stably infected with pcDNA3.1-LINC00261 or pcDNA3.1-NC in 0.2 ml of normal saline were injected in subcutaneous area of nude mice (n=3). The tumors were measured with a caliper once 1 week, and tumor volume was calculated using the formula: V (mm^3) = 1/2 ab^2 (a - the longest tumor axis, b - the shortest tumor axis). The mice were practiced with euthanasia on week 4 after xenograft and the weight of tumors was evaluated with electronic balance.

Statistical analyses. Data were presented as mean ± standard error of mean (SEM). A Student's *t*-test was performed to compare the differences between treated groups relative to their paired controls. Statistical analyses were performed using Graphpad, version 5.0 (GraphPad Software, Inc., La Jolla, USA) and *P*-values indicated in the figures were considered to be statistically significant compared with a value < 0.05. The statistical associations between expressions of LINC00261, miR-19a and KLF2 mRNA were evaluated with regression correlation analyses. Spearman's two-tailed correlation test and the two-tailed chi-square test were used for clinicopathological features. Kaplan-Meier analysis demonstrated the association between LINC00261 expression and overall survival rate.

Results

LINC00261 was downregulated in NSCLC and this expression was correlated with advanced tumor progression and poor prognosis. First of all, we detected the role of LINC00261 in NSCLC. RT-qPCR data showed LINC00261 was significantly downregulated (Figure 1A) in NSCLC tumors compared with paired adjacent normal tissues, and relative expression levels of

LINC00261 were distinctively lower in NSCLC cell lines A549, H1299, SK-MES-1, and PC-9 than normal human bronchial epithelium cell line BEAS-2B (Figure 1B). In addition, the patients recruited were divided into 2 groups: LINC00261 high expression (higher than mean, n=30) and LINC00261 low expression (lower than mean, n=32) according to RT-qPCR data (Figure S1). Lower level of LINC00261 was associated with higher TNM stage, larger tumor size and lymph node metastasis (Table 1). As shown in Figure 1C, the 5-year overall survival rate of NSCLC patients with LINC00313 high expression was appropriate 60%, and that of LINC00313 low expression was about 30%. These data showed that LINC00261 was downregulated in NSCLC and this expression was associated with advanced tumor progression, lymph node metastasis and poor prognosis among NSCLC patients.

Overexpression of LINC00261 suppressed NSCLC tumor cell progression *in vitro* and *in vivo*. Considering that LINC00261 was low expressed in NSCLC cells, and A549 and H1299 cells exhibited the lowest level of LINC00261 (Figure 1B), we forced LINC00261 highly expressed in A549 and H1299 cells by transfection. The high transfection efficiency was confirmed by RT-qPCR analyzing LINC00261 expression levels (Figure 2A). Then, a series of gain-of-function experiments were carried out. Cell viability of A549 and H1299 cells was measured using MTT assay, and pcDNA3.1-LINC00261 transfection caused declined OD450 values in 48-72 h compared with pcDNA-3.1-NC transfection (Figure 2B and 2C). Moreover, the tumorigenesis of A549 cells *in vivo* was measured after transfection. As Figure 2D depicted, xenograft tumor volumes were significantly smaller by highly expressed LINC00261 after transplantation for 3-4 weeks. The tumor weight was also declined in LINC00261 overexpression group (Figure 2E). The apoptosis was evaluated by flow cytometry and western blotting. As a result, apoptotic cells were statistically increased in cells transfected with pcDNA3.1-LINC00261, accompanied with higher level of Bax and cleaved caspase3, and lower level of Bcl-2 (Figure 2F and 2G). Transwell assays suggested that migrated cells and invaded cells were decreased by ectopic LINC00261 (Figure 2H and 2I). These results presented that upregulation of LINC00261 could promote NSCLC cell apoptosis, and inhibit cell viability, tumor growth, migration, and invasion in A549 and H1299 cells, suggesting the tumor-suppressive role of LINC00261 in NSCLC.

LINC00261 negatively regulated miR-19a by sponging and vice versa. A possible target gene of LINC00261 was retrieved and identified as miR-19a on miRcode website (Figure 3A). The

sequences of the putative binding site in LINC00261-3' UTR wild type were mutated as AGUUCGG. To confirm this, a dual-luciferase reporter assay was performed. And, Figure 3B showed that relative luciferase activity of LINC00261 wild type was dropped in HEK293T cells when transfected with miR-19a mimics; whereas there was little influence of LINC00261 mutant whenever transfected with miR-19a mimics or miR-NC mimics. Expression of miR-19a was measured in NSCLC tumors. Expectedly, miR-19a levels were upregulated and negatively liner correlated with LINC00261 level in NSCLC tumors (Figure 3C and 3D). In addition, the basic expression level of this miRNA was monitored in NSCLC cell lines, and the regulatory relationship between LINC00261 and miR-19a was determined. We observed miR-19a level was overall higher in A549, H1299, SK-MES-1, and PC-9 cells than the control cell line BEAS-2B (Figure S2), and was decreased in A549 and H1299 cells when transfected with pcDNA3.1-LINC00261 (Figure 3E) and increased when transfected with si-LINC00261 (Figure 3F); moreover, LINC00261 levels were also inversely regulated by miR-19a (Figure 3G and 3H). Taken together, our data proposed that there was a negative regulatory relationship between expressions of LINC00261 and miR-19a in NSCLC cells via target binding.

Upregulation miR-19a could abolish the tumor-suppressive role of LINC00261 in NSCLC cells *in vitro*. What's wondered us was that whether miR-19a expression in turn affect LINC00261 role in NSCLC cells. Rescue experiments were performed in A549 and H1299 cells when co-transfected with pcDNA3.1-LINC00261 and miR-19a mimics or miR-NC mimics. First and foremost, the diminished miR-19a expression mediated by LINC00261 overexpression was improved in the presence of miR-19a mimics (Figure 4A). A549 and H1299 cells co-transfected with pcDNA3.1-LINC00261 and miR-NC mimics showed lower cell viability than cells either transfected with pcDNA3.1-NC or co-transfected with pcDNA3.1-LINC00261 and miR-19a mimics (Figure 4B and 4C). Apoptosis rate and expression of Bax-2 and cleaved caspase 3 were elevated by pcDNA3.1-LINC00261, which was then blocked by miR-19a mimics (Figure 4D and 4E). Moreover, LINC00261 overexpression-induced inhibition on migrated cells and invaded cells was partially reversed by miR-19a upregulation (Figure 4F and 4G). These outcomes indicated that upregulation of miR-19a could abolish the effect of LINC00261 overexpression on NSCLC cell viability, apoptosis, migration and invasion in A549 and H1299 cells.

KLF2 was targeted and downregulated by miR-19a in NSCLC cells. This study observed a

potential binding site between miR-19a and KLF2 3'-UTR as predicted on Targetscan website (Figure 5A). The KLF2 3'-UTR wild type containing the putative miR-19a target site and its corresponding mutant were cloned into luciferase reporter plasmid pGL4 and relative luciferase activity of KLF2 wild type was dramatically decreased in HEK293T cells when transfected with miR-19a mimics (Figure 5B); meanwhile, there was no difference in KLF2 mutant groups. As demonstrated in Figure 5C, expression of KLF2 mRNA was downregulated in NSCLC tumors, and there existed a negative liner correlation between KLF2 mRNA expression and miR-19a expression (Figure 5D). In A549 and H1299 cells, KLF2 protein expression was downregulated when transfected with miR-19a mimics, and upregulated when expressed miR-19a inhibitors (Figure 5E and 5F). These data showed KLF2 was low expressed in NSCLC tumors and served as a downstream target for miR-19a in NSCLC cells.

Downregulation of KLF2 partially reversed the tumor-suppressive role of LINC00261 in NSCLC cells *in vitro* though miR-19a. According to the results, we hypothesized LINC00261/miR-19a/KLF2 pathway might contribute to NSCLC tumor cell progression. To further identify this, the impact of KLF2 expression on LINC00261 effect in NSCLC cells was measured. First of all, we detected KLF2 mRNA expression in NSCLC tumors, and found its expression was positively correlated with LINC00261 expression in a liner manner (Figure 6A). In vitro, KLF2 mRNA levels were upregulated by pcDNA3.1-LINC00261 transfection, and then were attenuated in the presence of miR-19a mimics or si-KLF2 (Figure 6B and 6C). Functionally, si-KLF2 rescued the inhibition of LINC00261 on cell viability (Figure 6D and 6E), migration and invasion (Figure 6H and 6I), and attenuated LINC00261-mediated sensitivity to apoptosis (Figure 6F and 6G) as evidenced by decreased apoptosis rate and expression of Bax and cleaved caspase 3. These results revealed that downregulation of KLF2 partially reversed the tumor-suppressive role of LINC00261 in NSCLC cells *in vitro*.

Discussion

LINC00261 functions as a tumor suppressor in lung cancer. LINC00261 was significantly downregulated in NSCLC, and its biological role in the progression of NSCLC was declared in several researches. For example, Liu *et al.* [11] showed for the first time that LINC00261 expression was associated with poor prognosis of NSCLC patients and might serve as an

independent prognostic indicator as evidenced by the association between low expression of LINC00261 and advanced TNM stage, poor lymph node status, and distant metastasis. Later, Dhamija *et al.* [14] also reported LINC00261 low expression was associated with recurrence and poor patient survival in lung adenocarcinoma. Moreover, they discovered that LINC00261 was strongly repressed in TGFβ-induced EMT in A549 and Calu-6 cells, as well as in the fast migrating lung cancer cell line NCI-H2030 compared to the slow migrating cell line NCI-H1993; on the contrary, LINC00261 expression was higher in the epithelial cluster of lung cancer cell lines. Therefore, it was suggested that LINC00261 as epithelial marker associated with lower cell migration potential in lung cancer cells. Soon, Liao *et al.* [16] announced that LINC00261 in turn inhibited EMT in NSCLC cells *in vitro*. Very recently, Shahabi *et al.* [15] explored the outcomes of LINC00261 reintroduction in lung adenocarcinoma cell line H522 and demonstrated inhibited cell migration, G2/M cell cycle, and tumor growth, while induced DNA damage pathway genes such as ATM kinase and TOP2A DNA helicase; knockdown of LINC00261 in A549 cells caused obviously increased cell proliferation, colony formation, invasion, but not migration, which was inconsistent with results from Liao *et al.* [16]. In this study, we supported the negative correlation between LINC00216 expression level and clinical symptoms TNM stage, tumor size, lymph node metastasis, and overall survival. The expression of LINC00261 was abundantly lower in NSCLC tumor tissues than the adjacent normal tissues. The tumor-suppressive effects of LINC00261 were noticed to be similar to previous studies on cell viability, migration, invasion, tumor growth, and apoptosis. To our best knowledge, our study firstly uncovers the influence of LINC00261 expression level on apoptosis in NSCLC cells *in vitro*, and it was suggested that LINC00261 overexpression enhanced apoptosis rate and expression of apoptosis-related gene Bax and cleaved caspase 3 in A549 and H1299 cells. Taken together, LINC00261 functions as a tumor suppressor in NSCLC cells inhibiting the tumor cell progression and correlating with good prognosis. The mechanisms underlying that include targeting Snail [16] and co-regulating with its neighbor gene FOXA2 [14, 15] via G2/M DNA damage checkpoint signaling, GADD45, RAN signaling, and *etc*. Here, we concluded that targeting miR-19a/KLF2 axis was a novel molecular pathway of LINC00261 in NSCLC cells (Figure S3). However, the key signaling pathways under LINC00261/miR-19a/KLF2 axis remain to be further investigated.

It is well-documented that LINC00261 exhibited anti-tumor role in different cancers, even

though the investigations focused on LINC00261 remain very limited so far. LINC00261-associated ceRNA net has been gradually establishing including LINC00261/miR-132-3p/BCL2L11 in endometriosis [23], LINC00261/miR-558/TIMP4 in pre-eclampsia [24], LINC00261/miR-182, miR-183, miR-153, miR-27a, and miR-96/FOXO1 in endometrial carcinoma [20], and LINC00261/miR-19a/KLF2 in NSCLC (Figure S3). More and further LINC00261/miRNAs/mRNAs pathways should be revealed in cancers such as lung cancer.

miR-19a is a key oncogenic member of miR-17-92 family, a highly conserved gene cluster. Mechanically, on one hand, miR-19a was regulated by several lncRNA sponges to exert its oncogenic functions. There are several lncRNAs identified as sponge for miR-19a in gastric cancer and breast cancer. For instance, lncRNAs-SLC25A5-AS1 decreased cell proliferation and increased cell apoptosis via directly downregulating miR-19a expression [25]; downregulated lncRNA-CASC2 contributed to the development of cisplatin resistance through targeting miR-19a [26]. Wu *et al.* [27] speculated that miR-19a might be co-expressed with lncRNA-DLEU1 to co-regulate the expression of ESR1, which influences the occurrence and development of breast cancer MCF-7 and MDA-MB-231 cells. Moreover, lncRNAs-H19 and -AP000288.2 were predicted by miRcode website to interact with miR-19a [28], whereas this has not been further confirmed yet. In lung cancer, there is one lncRNA is clear to sponge this miRNA before this present study. Xing *et al.* [29] proposed low expression of lncRNA-AC078883.3 and miR-19a was involved in cisplatin resistance in NSCLC A549 and H460 cells. In this study, we discovered LINC00261 targeting miR-19a could promote NSCLC cell apoptosis, and inhibit cell viability, migration, invasion, and tumor growth in A549 and H1299 cells.

On the other hand, miR-19a targeted many downstream genes and pathways to exert its oncological effects. miR-19a is highly expressed in malignant lung cancer cells and is considered the key miRNA for tumorigenesis of NSCLC. Furthermore, direct targets of miR-19a including FOXP1, TP53INP1, TNFAIP3, and TUSC2 in regulating lung cancer cell progression had been uncovered [30]. Among the discovered genes on Targetscan database, KLF2 is a novel potential target for miR-19a. KLF2 belongs to Kruppel-like factor family and also known as lung Kruppel-like factor [31]. KLF2 has been suggested to be a tumor suppressor in cancers, especially in NSCLC [32]. Its expression was higher in embryo and adult normal lung tissues [33]; however, KLF2 was frequently lower expressed in various cancer tissues during which it could induce

apoptosis and inhibit cell proliferation, migration and angiogenesis [34, 35]. In consideration of the vital role of KLF2 in NSCLC, thus we wondered whether existed a miR-19a/KLF2 axis in A549 and H1299 cells. Luciferase reporter assay confirmed the complementary binding between miR-19a and KLF2. Moreover, the negative regulatory relationship of miR-19a on KLF2 protein was discovered as well. Expression of KLF2 mRNA was significantly downregulated in tumor tissues from NSCLC patients in an inverse liner correlation with miR-19a and a positive liner correlation with LINC00261 expression. Furthermore, expression of miR-19a was inhibited and KLF2 was enhanced in mice NSCLC tumors induced by LINC00261-overexpressed A549 cells (Figure S4). Mechanically, LINC00261 showed its tumor-suppressive role in NSCLC cells through upregulating KLF2 via targeting miR-19a. Most of important, our work indicated KLF2 functioned as a downstream target of LINC00261/miR-19a in NSCLC.

In conclusion, we demonstrate that LINC00261 is downregulated in NSCLC, which is involved in higher TNM stage, larger tumor size, lymph node metastasis, and poor prognosis. Upregulation of LINC00261 could promote NSCLC cell apoptosis, and inhibit cell viability, tumor growth, migration, and invasion in A549 and H1299 cells. Our results suggest that LINC00261 could suppress NSCLC tumor cell progression *in vitro* and *in vivo* through LINC00261/miR-19a/KLF2 pathway. This work can provide a novel knowledge and approach for the initiation, development and prognosis in NSCLC.

References

[1] ZHONG H, SIDDIQUI SM, MOVSAS B, CHETTY IJ. Evaluation of adaptive treatment planning for patients with non-small cell lung cancer. Phys Med Biol 2017; 62: 4346-4360. https://doi.org/10.1088/1361-6560/aa586f

[2] BRAY F, FERLAY J, SOERJOMATARAM I, SIEGEL RL, TORRE LA et al. Global cancer statistics 2018: GLOBOCAN estimates of incidence and mortality worldwide for 36 cancers in 185 countries. CA Cancer J Clin 2018; 68: 394-424. https://doi.org/10.3322/caac.21492

[3] ALLEMANI C, WEIR HK, CARREIRA H, HAREWOOD R, SPIKA D et al. Global surveillance of cancer survival 1995-2009: analysis of individual data for 25,676,887 patients from 279 population-based registries in 67 countries (CONCORD-2). Lancet 2015; 385: 977-1010. https://doi.org/10.1016/S0140-6736(14)62038-9

[4] DENG D, LIU L, XU G, GAN J, SHEN Y et al. Epidemiology and serum metabolic characteristics of acute myocardial infarction patients in chest pain centers. Iran J Public Health 2018; 47: 1017-1029.

[5] PENG Z, ZHANG C, DUAN C. Functions and mechanisms of long noncoding RNAs in lung cancer. Onco Targets Ther 2016; 9: 4411-4424. https://doi.org/10.2147/OTT.S109549

[6] LI CH, CHEN Y. Targeting long non-coding RNAs in cancers: progress and prospects. Int J Biochem Cell Biol 2013; 45: 1895-1910. https://doi.org/10.1016/j.biocel.2013.05.030

[7] WEI MM, ZHOU GB. Long Non-coding RNAs and their roles in non-small cell lung cancer. Genomics Proteomics Bioinformatics 2016; 14: 280-288. https://doi.org/10.1016/j.gpb.2016.03.007

[8] ONG SB, KATWADI K, KWEK XY, ISMAIL NI, CHINDA K et al. Non-coding RNAs as therapeutic targets for preventing myocardial ischemia-reperfusion injury. Expert Opin Ther Targets 2018; 22: 247-261. https://doi.org/10.1080/14728222.2018.1439015

[9] ZHOU D, XIE M, HE B, GAO Y, YU Q et al. Microarray data re-annotation reveals specific lncRNAs and their potential functions in non-small cell lung cancer subtypes. Mol Med Rep 2017; 16: 5129-5136. https://doi.org/10.3892/mmr.2017.7244

[10] LU T, WANG Y, CHEN D, LIU J, JIAO W. Potential clinical application of lncRNAs in non-small cell lung cancer. Onco Targets Ther 2018; 11: 8045-8052. https://doi.org/10.2147/OTT.S178431

[11] LIU Y, XIAO N, XU SF. Decreased expression of long non-coding RNA LINC00261 is a prognostic marker for patients with non-small cell lung cancer: a preliminary study. Eur Rev Med Pharmacol Sci 2017; 21: 5691-5695.

[12] LIN K, JIANG H, ZHUANG SS, QIN YS, QIU GD et al. Long noncoding RNA LINC00261 induces chemosensitization to 5-fluorouracil by mediating methylation-dependent repression of DPYD in human esophageal cancer. FASEB J 2019; 33: 1972-1988. https://doi.org/10.1096/fj.201800759R

[13] YU Y, LI L, ZHENG Z, CHEN S, CHEN E et al. Long non-coding RNA linc00261 suppresses gastric cancer progression via promoting Slug degradation. J Cell Mol Med 2017; 21: 955-967. https://doi.org/10.1111/jcmm.13035

[14] DHAMIJA S, BECKER AC, SHARMA Y, MYACHEVA K, SEILER J et al. and the adjacent gene are epithelial markers and are suppressed during lung cancer tumorigenesis and progression. Noncoding RNA 2018; 5. https://doi.org/10.3390/ncrna5010002

[15] SHAHABI S, KUMARAN V, CASTILLO J, CONG Z, NANDAGOPAL G et al. LINC00261 Is an Epigenetically Regulated Tumor Suppressor Essential for Activation of the DNA Damage Response. Cancer Res 2019; 79: 3050-3062. https://doi.org/10.1158/0008-5472.CAN-18-2034

[16] LIAO J, DONG LP. Linc00261 suppresses growth and metastasis of non-small cell lung cancer via repressing epithelial-mesenchymal transition. Eur Rev Med Pharmacol Sci 2019; 23: 3829-3837. https://doi.org/10.26355/eurrev_201905_17810

[17] TAM C, WONG JH, TSUI SKW, ZUO T, CHAN TF et al. LncRNAs with miRNAs in regulation of gastric, liver, and colorectal cancers: updates in recent years. Appl Microbiol Biotechnol 2019; 103: 4649-4677. https://doi.org/10.1007/s00253-019-09837-5

[18] GUO T, LI J, ZHANG L, HOU W, WANG R et al. Multidimensional communication of microRNAs and long non-coding RNAs in lung cancer. J Cancer Res Clin Oncol 2019; 145: 31-48. https://doi.org/10.1007/s00432-018-2767-5

[19] ZHANG S, CAO R, LI Q, YAO M, CHEN Y et al. Comprehensive analysis of lncRNA-associated competing endogenous RNA network in tongue squamous cell carcinoma. PeerJ 2019; 7: e6397. https://doi.org/10.7717/peerj.6397

[20] FANG Q, SANG L, DU S. Long noncoding RNA LINC00261 regulates endometrial carcinoma progression by modulating miRNA/FOXO1 expression. Cell Biochem Funct 2018; 36: 323-330. https://doi.org/10.1002/cbf.3352

[21] PI J, TAO T, ZHUANG T, SUN H, CHEN X et al. A MicroRNA302-367-Erk1/2-Klf2-S1pr1 pathway prevents tumor growth via restricting angiogenesis and improving vascular stability. Circ Res 2017; 120: 85-98. https://doi.org/10.1161/CIRCRESAHA.116.309757

[22] LI J, YANG S, YAN W, YANG J, QIN YJ et al. MicroRNA-19 triggers epithelial-mesenchymal transition of lung cancer cells accompanied by growth inhibition. Lab Invest 2015; 95: 1056-1070. https://doi.org/10.1038/labinvest.2015.76

[23] WANG H, SHA L, HUANG L, YANG S, ZHOU Q et al. LINC00261 functions as a competing endogenous RNA to regulate BCL2L11 expression by sponging miR-132-3p in endometriosis. Am J Transl Res 2019; 11: 2269-2279.

[24] CHENG D, JIANG S, CHEN J, LI J, AO L et al. Upregulated long noncoding RNA Linc00261 in pre-eclampsia and its effect on trophoblast invasion and migration via regulating miR-558/TIMP4 signaling pathway. J Cell Biochem 2019; 120: 13234-13253. https://doi.org/10.1002/jcb.28598

[25] LI X, YAN X, WANG F, YANG Q, LUO X et al. Down-regulated lncRNA SLC25A5-AS1 facilitates cell growth and inhibits apoptosis via miR-19a-3p/PTEN/PI3K/AKT signalling pathway in gastric cancer. J Cell Mol Med 2019; 23: 2920-2932. https://doi.org/10.1111/jcmm.14200

[26] LI Y, LV S, NING H, LI K, ZHOU X et al. Down-regulation of CASC2 contributes to cisplatin resistance in gastric cancer by sponging miR-19a. Biomed Pharmacother 2018; 108: 1775-1782. https://doi.org/10.1016/j.biopha.2018.09.181

[27] WU Q, GUO L, JIANG F, LI L, LI Z et al. Analysis of the miRNA-mRNA-lncRNA networks in ER+ and ER- breast cancer cell lines. J Cell Mol Med 2015; 19: 2874-2887. https://doi.org/10.1111/jcmm.12681

[28] XIA T, LIAO Q, JIANG X, SHAO Y, XIAO B et al. Long noncoding RNA associated-competing endogenous RNAs in gastric cancer. Sci Rep 2014; 4: 6088. https://doi.org/10.1038/srep06088

[29] XING S, QU Y, LI C, HUANG A, TONG S et al. Deregulation of lncRNA-AC078883.3 and microRNA-19a is involved in the development of chemoresistance to cisplatin via modulating signaling pathway of PTEN/AKT. J Cell Physiol 2019; 234: 22657-22665. https://doi.org/10.1002/jcp.28832

[30] YAMAMOTO K, ITO S, HANAFUSA H, SHIMIZU K, OUCHIDA M. Uncovering direct targets of mir-19a involved in lung cancer progression. PLoS One 2015; 10: e0137887. https://doi.org/10.1371/journal.pone.0137887

[31] PEARSON R, FLEETWOOD J, EATON S, CROSSLEY M, BAO S. Krüppel-like transcription factors: a functional family. Int J Biochem Cell Biol 2008; 40: 1996-2001. https://doi.org/10.1016/j.biocel.2007.07.018

[32] JIANG W, XU X, DENG S, LUO J, XU H et al. Methylation of Kruppel-like factor 2 (KLF2) associates with its expression and non-small cell lung cancer progression. Am J Transl Res 2017; 9: 2024-2037

[33] BUCKLEY AF1, KUO CT, LEIDEN JM. Transcription factor LKLF is sufficient to program T cell quiescence via a c-Myc-dependent pathway. Nat Immunol 2001; 2: 698-704. https://doi.org/10.1038/90633

[34] YIN L, WANG JP, XU TP, CHEN WM, HUANG MD et al. Downregulation of Kruppel-like factor 2 is associated with poor prognosis for nonsmall-cell lung cancer. Tumour Biol 2015; 36: 3075-3084. https://doi.org/10.1007/s13277-014-2943-4

[35] KOBUS K, KOPYCINSKA J, KOZLOWSKA-WIECHOWSKA A, URASINSKA E, KEMPINSKA-PODHORODECKA A et al. Angiogenesis within the duodenum of patients with cirrhosis is modulated by mechanosensitive Kruppel-like factor 2 and microRNA-126. Liver Int 2012; 32:1222-1232. https://doi.org/10.1111/j.1478-3231.2012.02791.x

Figure legends

Figure 1. Expression of lncRNA-LINC00261 (LINC00261) in non-small cell lung cancer (NSCLC). A) Levels of LINC00261 in paired NSCLC tumor tissues (n=62) and normal tissues (n=62) were detected by RT-qPCR. B) Levels of LINC00261 in human NSCLC cell lines (A549, H1299, SK-MES-1, and PC-9) and normal human bronchial epithelium (BEAS-2B) were detected by RT-qPCR. C) The Kaplan-Meier curve of NSCLC patients with different expression of LINC00261. All experiments were carried out in 3 times, and $^{**}P < 0.01$.

Figure 2. Effects of LINC00261 knockdown in NSCLC cells *in vitro* and *in vivo*. A549 and H1299 cells were transfected with pcDNA3.1-LINC00261/NC. A) Expressions of LINC00261 were detected by RT-qPCR after transfection for 48 h. B and C) Cell viability was measured using MTT assay after transfection for 0, 24, 48, and 72 h. D and E) Stably transfected A549 cells were subcutaneously injected into BCLA/c mice (male, n=3) and xenograft tumors were generated. D) Tumor volume was monitored every week and tumor growth curve was drawn. E) The tumor weight was determined on week 4. After transfection for 48 h apoptotic cells was examined on flow cytometry (G), expressions of cleaved caspase 3, Bax and Bcl-2 were detected with western blotting (H), and migrated (I) and invaded (J) cells were showed by transwell assays. All experiments were carried out in 3 times, and $^{**}P < 0.01$.

Figure 3. LINC00261 negatively regulated miR-19a by sponging and vice versa. A) Prediction of the potential binding site of miR-19a on LINC00261 wild type (LINC00261-WT) on miRcode website. The putative targeting site was mutated as LINC00216-MUT. B) Relative luciferase activity was examined by luciferase reporter assay in HEK293T cells co-transfected with

miR-19a/NC mimics and LINC00261-WT or LINC00261-MUT. Expression of miR-19a (C) in paired NSCLC tumor tissues (n=62) and normal tissues (n=62) were detected and Spearman's correlation analysis depicted the association between expressions of miR-19a and LINC00261 (D). E and F) Expressions of miR-19a in A549 and H1299 cells were detected when transfected with pcDNA3.1-LINC00261, siRNA against LINC00261 (si-LINC00261), or its negative control. G and H) Expressions of LINC00261 in A549 and H1299 cells were measured when transfected with miR-19a mimics, miR-19a inhibitor, or its negative control. All experiments were carried out in 3 times, and $^{**}P < 0.01$.

Figure 4. Influence of miR-19a upregulation on the tumor-suppressive role of LINC00261 in NSCLC cells *in vitro*. A549 and H1299 cells were transfected with pcDNA3.1-NC, and co-transfected with pcDNA3.1-LINC00261 and miR-19a mimics or miR-NC mimics. A) Expressions of miR-19a were detected by RT-qPCR after transfection for 48 h. B and C) Cell viability were measured using MTT assay after transfection for 0, 24, 48, and 72 h. After transfection for 48 h apoptotic cells was examined on flow cytometry (D), expressions of cleaved caspase 3, Bax and Bcl-2 were detected with western blotting (E), and migrated (F) and invaded (G) cells were measured by transwell assays. All experiments were carried out in 3 times, and $^{*}P < 0.05$, $^{**}P < 0.01$, $^{****}P < 0.0001$.

Figure 5. miR-19a targeted and downregulated Kruppel-like factor 2 (KLF2) in NSCLC cells. A) The potential binding site between miR-19a and KLF2 wild type (KLF2-WT) was predicted on Targetscan website. The putative targeting site was mutated as KLF2-MUT. B) Relative luciferase activity of KLF2-WT/MUT was examined by luciferase reporter assay in HEK293T cells transfected with miR-19a/NC mimics. Expression of KLF2 mRNA in paired NSCLC tumor tissues (n=62) and normal tissues (n=62) were detected (C) and Spearman's correlation analysis depicted the association between expressions of miR-19a and KLF2 mRNA (D). E and F) Western blotting detected KLF2 protein expressions in A549 and H1299 cells when transfected with miR-19a mimics, miR-19a inhibitor, or its negative control. All experiments were carried out in 3 times, and $^{**}P < 0.01$.

Figure 6. Influence of KLF2 downregulation on tumor-suppressive role of LINC00261 in NSCLC cells *in vitro*. A) The positive correlation between expressions of LINC00261 and KLF2 mRNA in NSCLC tumor tissues was confirmed by Spearman's correlation analysis. B) Expression of KLF2 mRNA was measured by RT-qPCR in A549 and H1299 cells when transfected with pcDNA3.1-NC and co-transfected with pcDNA3.1-LINC00261 and miR-19a/NC mimics. C-I) A549 and H1299 cells were transfected with pcDNA3.1-NC and co-transfected with pcDNA3.1-LINC00261 and siRNA against KLF2 (si-KLF2) or scrambled siRNA (si-NC). C) Expression of KLF2mRNA was measured by RT-qPCR after transfection for 48 h. D and E) Cell viability were measured using MTT assay after transfection for 0, 24, 48, and 72 h. After transfection for 48 h apoptotic cells was examined on flow cytometry (F), expressions of cleaved caspase 3, Bax and Bcl-2 were detected with western blotting (G), and migrated (H) and invaded (I) cells were showed by transwell assays. All experiments were carried out in 3 times, and $*P < 0.05$, $**P < 0.01$, $****P < 0.0001$.

Supplementary Figure Legends

Figure S1. LINC00261 levels in 62 NSCLC patients.

Figure S2. Expression of miR-19a was upregulated in human NSCLC cell lines. RT-qPCR detected miR-19a levels in A549, H1299, SK-MES-1, and PC-9 cells, compared to that in normal human bronchial epithelium cell line BEAS-2B. $*P < 0.05$

Figure S3. LINC00261/miR-19a/KLF2 pathway participated in NSCLC tumor cell progression.

Figure S4. Xenograft tumors expressed higher LINC00261 and KLF2 levels, and lower miR-19a level. (A-C) RT-qPCR detected levels of LINC00261, miR-19a and KLF2 in tumor tissues from mice. $**P < 0.01$

560 **Table 1**. Correlation between the clinicopathologic characteristics and relative expression levels of

561 LINC00261 in the 62 patients with NSCLC

Parameters	LINC00261 expression		*P* value
	Low(n=32)	High(n=30)	
Age			0.712
≥65	19	20	
<65	13	10	
Gender			0.546
Female	11	8	
Male	21	22	
Smoking			0.641
No	15	11	
Yes	17	19	
TNM stage			0.023*
StageI	9	20	
StageII/III	23	10	
Tumor size			0.012*
≥5	18	9	
<5	14	21	
Lymph node metastasis			0.035*
No	12	17	
Yes	20	13	

562 NSCLC: non-small cell lung cancer; TNM stage: tumor, node, and metastasis stage.

563 *Statistically significant is in bold

564

Fig. 1 Download full resolution image

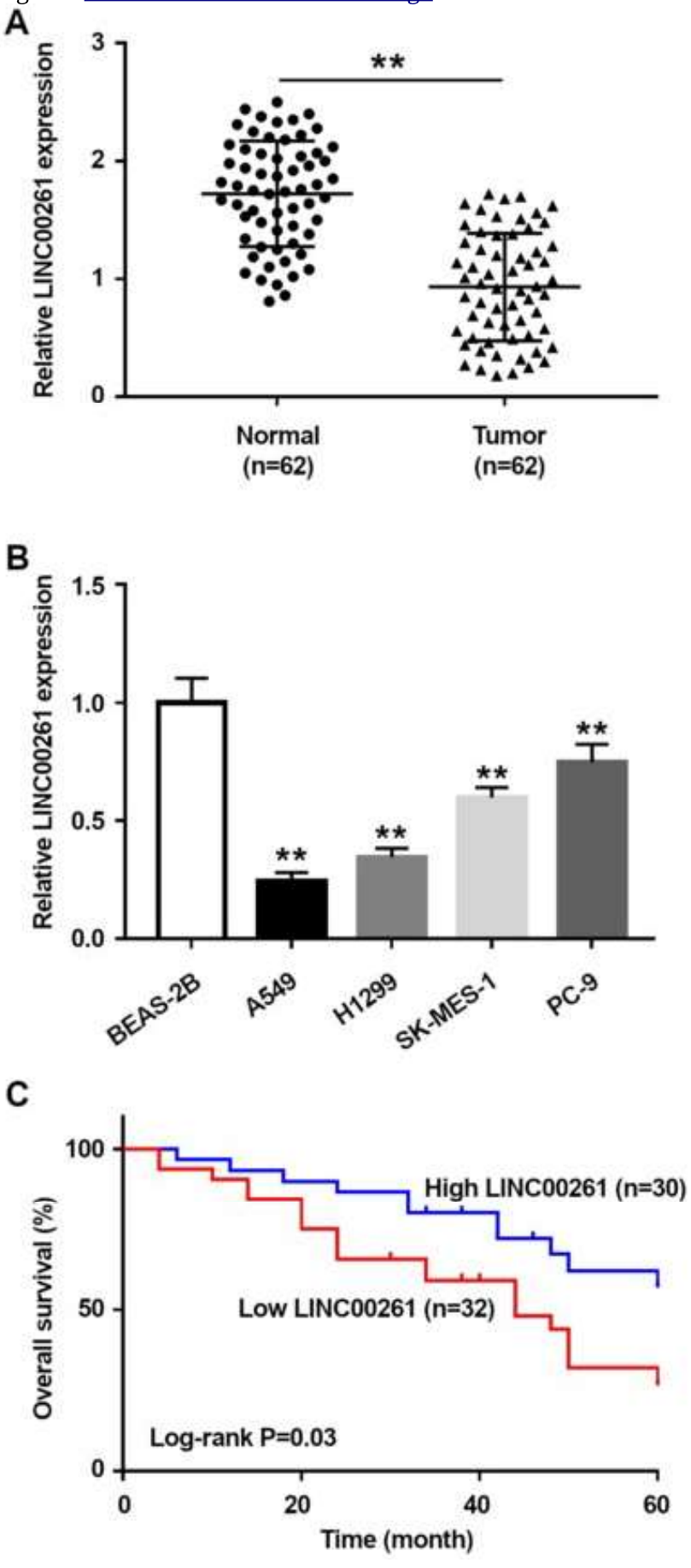

Fig. 2 [Download full resolution image]

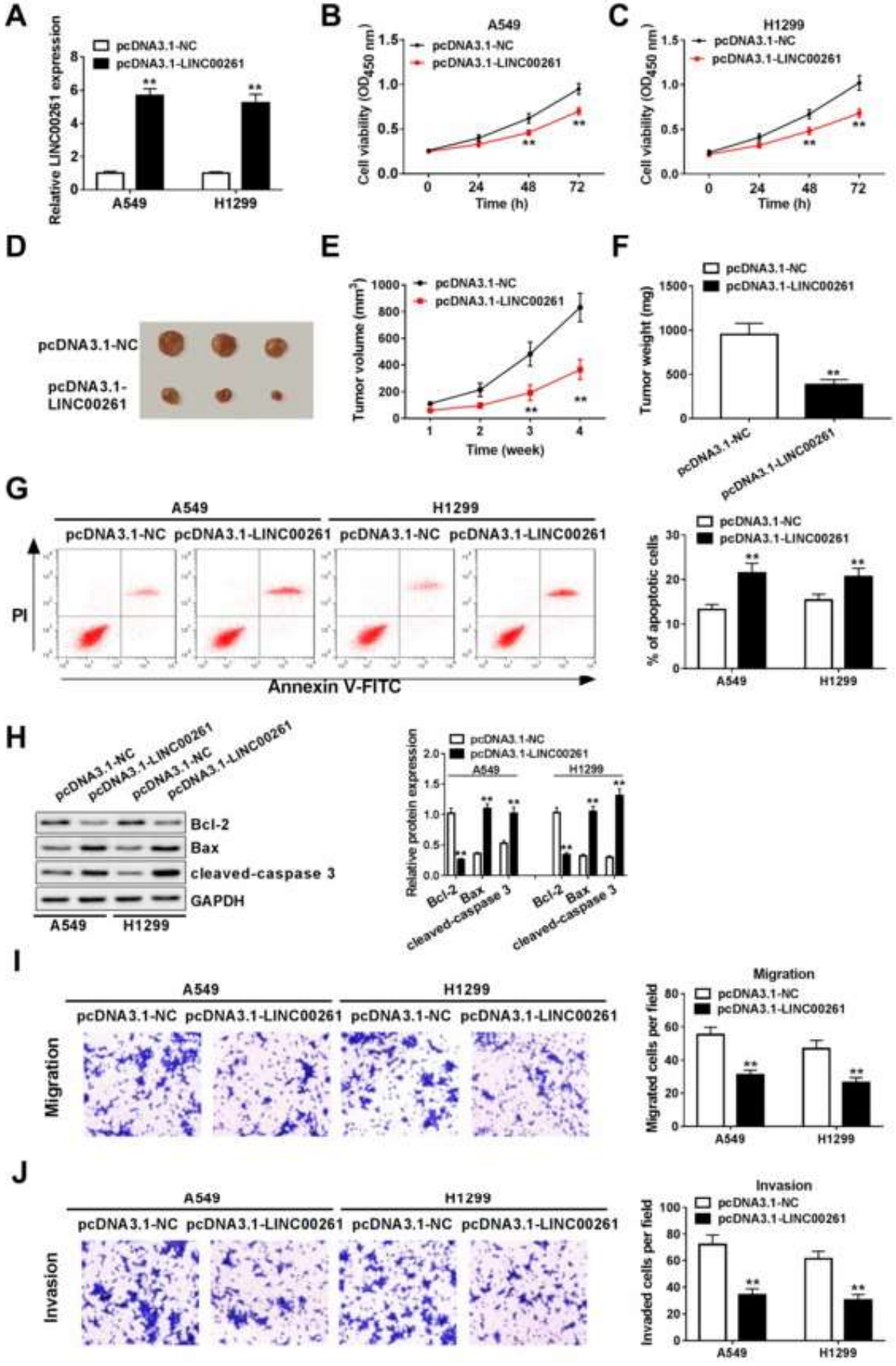

Fig. 3 Download full resolution image

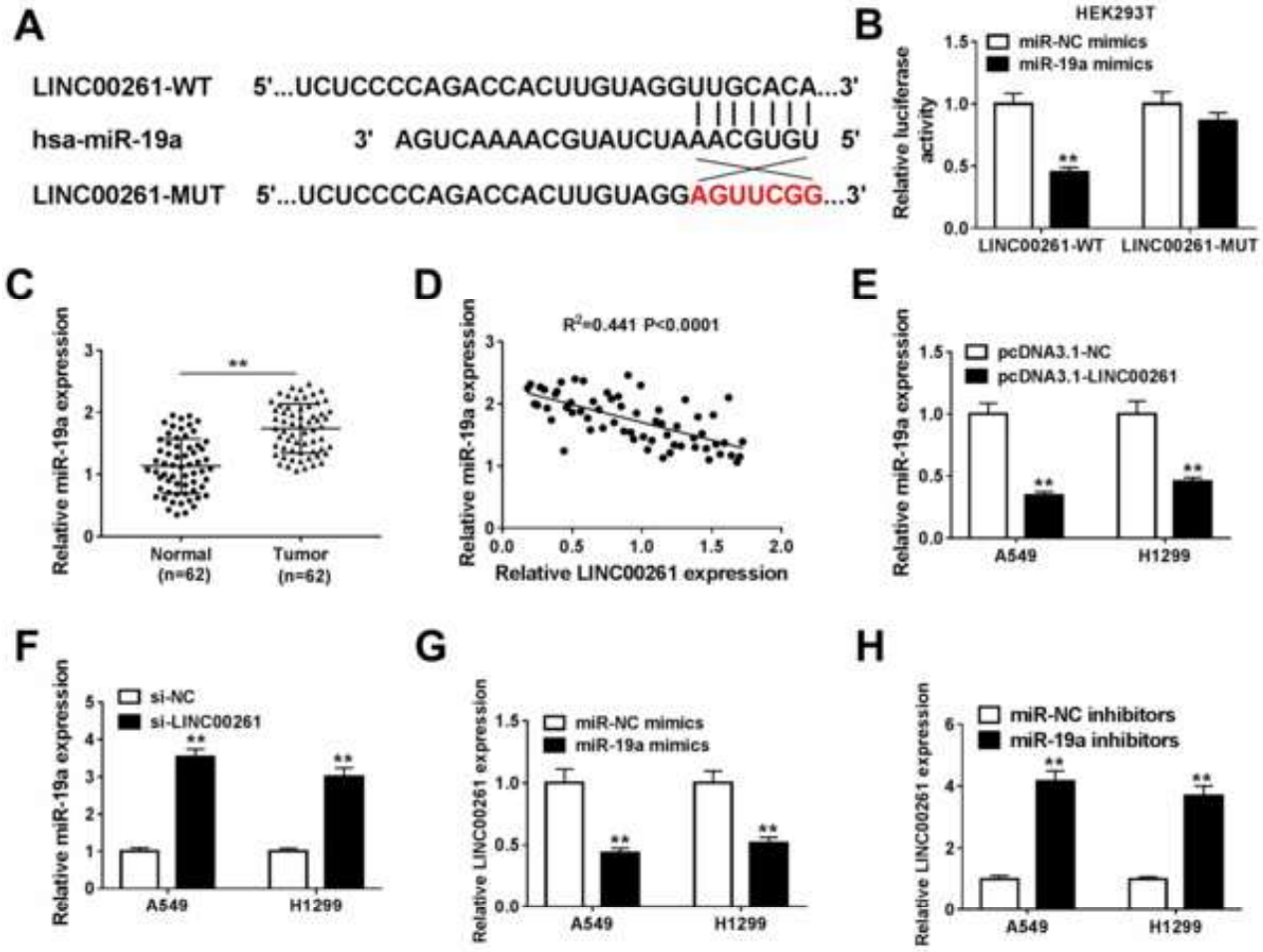

Fig. 4 Download full resolution image

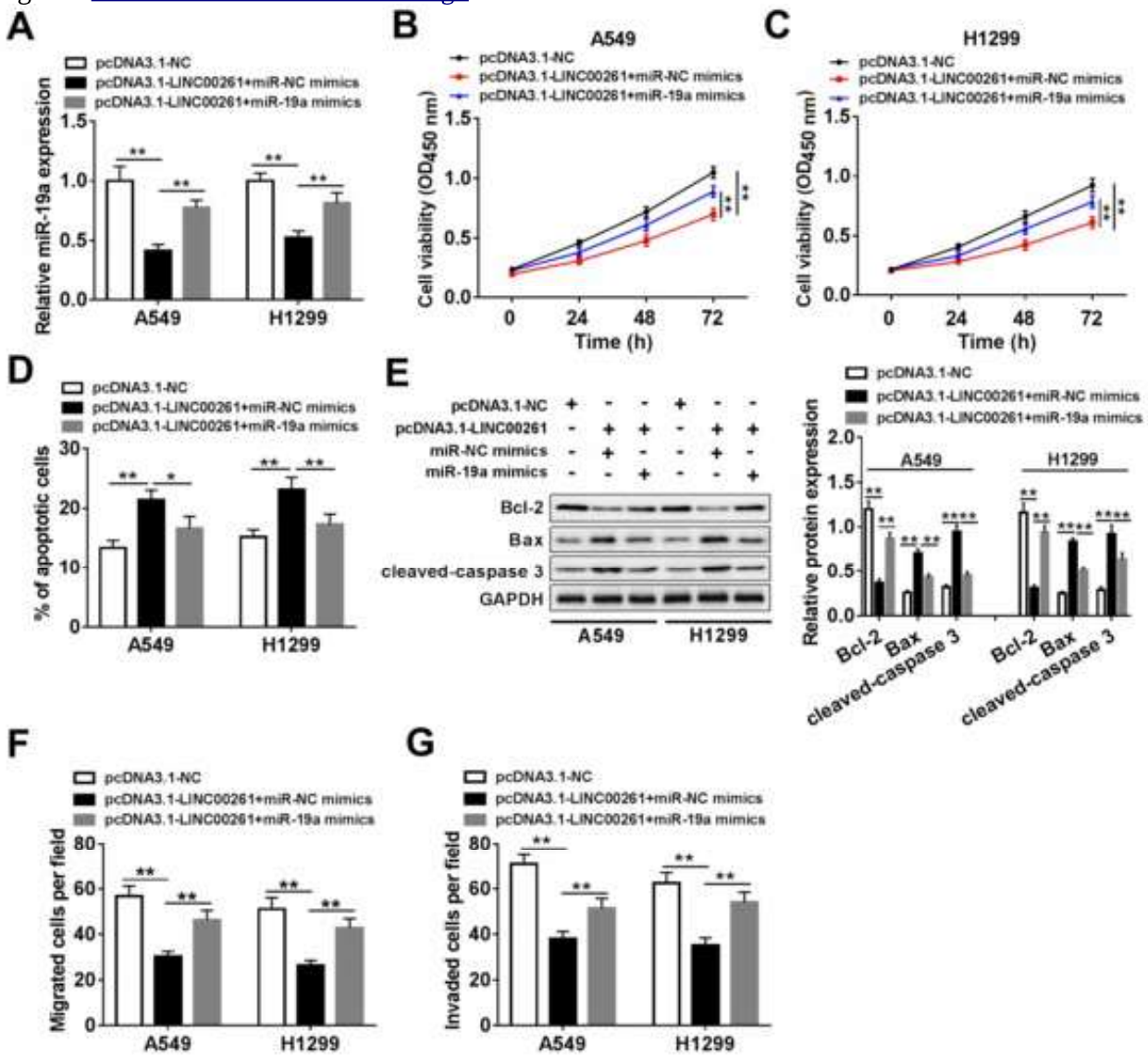

Fig. 5 Download full resolution image

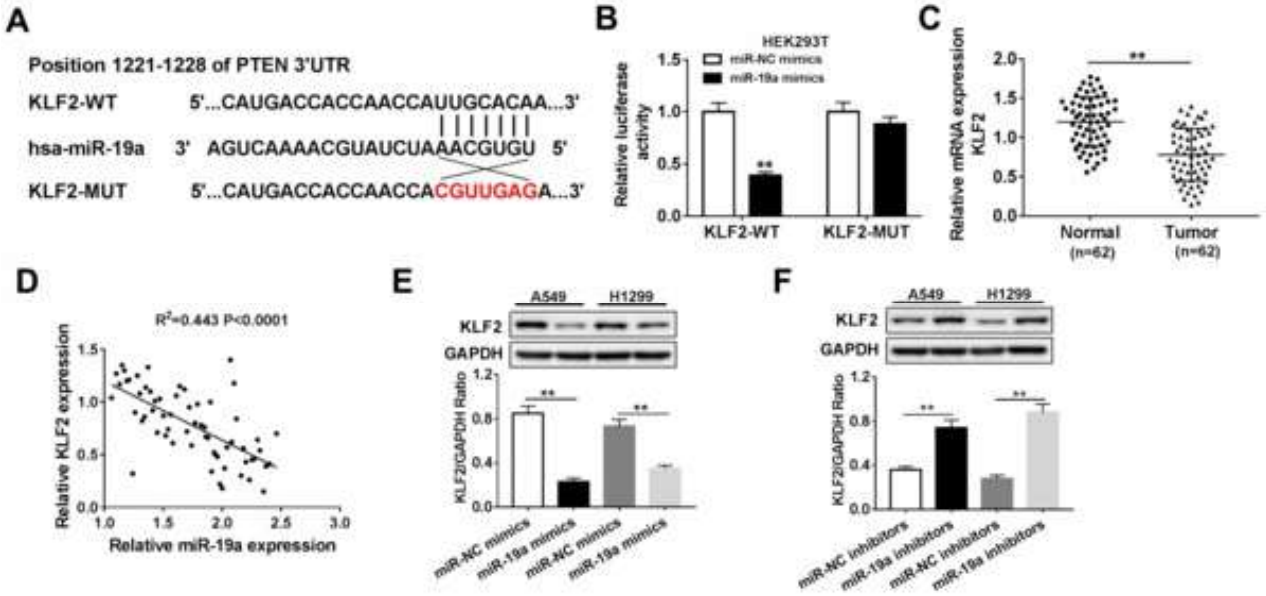

Fig. 6 Download full resolution image